Nigerian Research Journal of Engineering and Environmental Sciences 4(1) 2019 pp. 389-397

Nigerian Research Journal of Engineering and Environmental Sciences
Journal homepage: www.rjees.com

Original Research Article

Enhanced Photo-generated Carrier Transport in an Excitonic Photocell

Oduah, U.I.
Department of Physics, Faculty of Science, University of Lagos, Lagos, Nigeria.
uoduah@unilag.edu.ng

ARTICLE INFORMATION

Article history:
Received 28 January, 2019
Revised 04 March, 2019
Accepted 07 March, 2019
Available online 30 June, 2019

Keywords:
Magnetotactic bacteria
Solar cell
Photocell
Exciton
Photovoltaic

ABSTRACT

This paper proposes an enhanced photo-generated carrier transport mechanism in an excitonic photocell considering a novel process. The proposed photovoltaic device implements nanoparticles of magnetites isolated from magnetosomes of magnetotactic bacteria (MTB) for the efficient transport of excitons. By integrating nanoparticles of magnetite in the excitonic photocell, the overall efficiency and temperature stabilization of the device was enhanced. A panchromatic ruthenium complex sensitizer dye was applied to increase molar extinction coefficient in the solar cell. Applying Zinc Oxide (ZnO) nanowires an improved circulation of photo-generated carriers with trap diffusion was created maximizing transport efficiency. The developed device achieved a fill factor of 0.82 and overall efficiency of 13.2% attributed to the MTB. The availability of the device materials makes it feasible for mass production.

1. INTRODUCTION

The various technologies for the conversion of incident photons to electricity are limited by recombination losses associated with the lifetime of excitons (Mahmoud *et al.,* 2016). The existing organic photovoltaic cells include the planar two-layer solar cell introduced, the dye-sensitized solar cell (DSSC), and the bulk hetero-junction solar cell (Khan *et al.*, 2017). Although silicon offers efficiency up to about 30%, these limits are yet to be exceeded even with different modifications of the device (Peng *et al.,* 2018). Again, the high cost of fabrication of the silicon devices and the toxic chemicals associated with the production process are major drawbacks of silicon solar cells (Kruger *et al.*, 2003). Dye sensitized solar cells are designed to replicate the natural process by which chlorophyll traps sunlight during photosynthesis. The DSSC suffers limitations such as poor efficiency index, and complex production process leading to difficulty in commercialization (Change *et al.,* 2010). Considering the volume of research on silicon solar cells from inception to date and the currently achieved minimal operational efficiency compared to the sustained gradual growth in the DSSC efficiency, it is a good option to focus on DSSC technology. The features of DSSC are unique and advantageous compared to the solar cell devices that are based on crystalline or amorphous silicon (Naik *et al.*, 2017). One striking advantage of DSSC is the ability of the components to be tunable such as the semiconducting oxide substrate, the dye, the electrolytes, the redox mediator and the

counter electrodes. There are ongoing researches with various organic materials to position DSSC to be more competitive in the solar cell markets as noted by various studies (Naik *et al.,* 2018). The target is to improve on the incident photon conversion efficiency (IPCE), enhance the cell durability, and reduce the cost of production by applying an environmentally friendly technique. Several technologies have been used to improve on spectral absorbance by making modification in the dye, enhancing the carrier transport mechanism, replacement of the liquid electrolyte with conducting polymers or ionic solids and other engineering of the semiconductor bandgap architecture (Wadman *et al.,* 2011, Duerto *et al.,* 2018). Recent DSSC's are relatively low cost with nontoxic components that can easily be synthesized from abundant natural products.

2. MATERIALS AND METHODS

2.1. Materials

The magnetotactic bacteria were collected from the lagoon at University of Lagos using sample bottles. The nanoparticles of magnetites extracted from the magnetosomes of magnetotactic bacteria were used in the solar cell to achieve coherent transportation of the photo-generated carriers. ZnO nanowires of about 65 nm diameters and length of 10 µm were synthesized and applied as conducting channels for generated carriers. Ruthenium complex dye combined with the ZnO nanowires is a structure implemented to increase the light harvesting properties of the solar cell.

2.2. Operating Principles

The structure of the developed photocell is presented in Figure 1. This research introduces a novel unique excitonic photocell described in Figure 1. It consists of a conducting glass, a ruthenium dye as photo sensitizer, zinc oxide nanowires loaded with nanoparticles of magnetite isolated from magnetosomes of MTB as charge carrier and electrodes. The device structure is designed to perform two functions which are photon absorption and charge carrier transport. Photo excitation at the monolayer of the ruthenium dye results in the injection of electrons into the conduction band of the ZnO. The heart of this device is composed of meso-porous nanoparticles with aggregate pore width of 2.50 nm and an oxide layer which allows accelerated electronic conduction to occur.

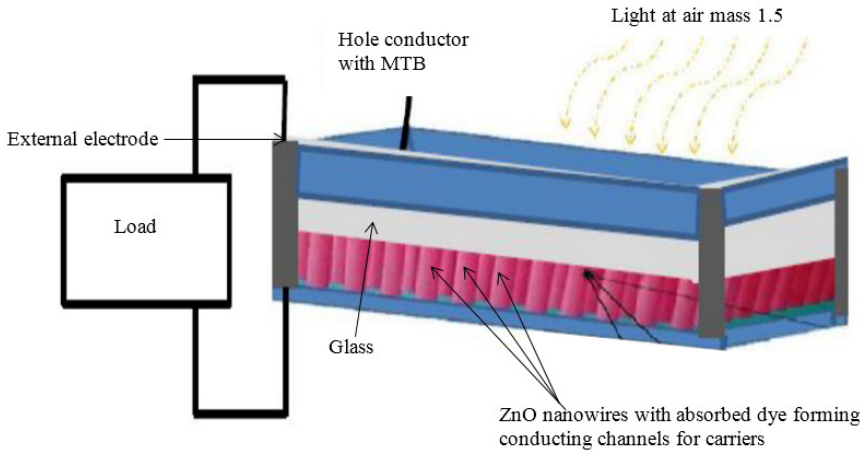

Figure 1: Developed excitonic photocell with enhanced carrier transport system

The uniqueness of this device is its characteristic photo-generated carriers transport mechanism in which excitons are accelerated by inbuilt magnetic field of nanoparticles of MTB. The speedy transport of excitons

will reduce the intrinsic recombination losses in this device which in turn enhances the overall power conversion efficiency (Benhattab *et al.,* 2018). Another desirable effect to be realized by incorporating the MTB in the device is that of temperature stability. This temperature stability is attributed to the coherent transportation of the photo-generated excitons in the excitonic photocell (Oduah and Yang, 2016). The steps taken in the processing of the materials to be used in the development of the DSSC are outlined as follows.

Samples of the MTB were collected from the Lagoon at University of Lagos, Nigeria, using screw top bottles. Then magnetic spirillum growth medium was used for the culture of the MTB. The culture method is according to the previous work (Zhu *et al.,* 2010). The magnetosomes of the MTB were then isolated and the crystal nanoparticles of the magnetite (Fe_3O_4) characterized using selected area electron diffraction (SAED) forms. Applying ionic interaction, the substrate was incorporated with isolated nanoparticles of the crystal magnetite. Transmission electron microscopy and Zeta potential were then used for the characterization of the magnetite nanoparticles. The processes deployed in the isolation and characterization of the nanoparticles of magnetite described above follow the previous experimental protocols (Atlas *et al.,* 2010; Jobin *et al.,* 2016). The characterization of the developed solar cell was achieved by connecting the output of the solar cell to Labview toolkit VI software in a computer laptop.

2.3. The ZnO Nanowires

Nanowires of ZnO are to be used as photoanode of the proposed solar cell. Nanowires of about 65nm diameter and length of 10 µm were synthesized using substrate of Fluorine tin oxide (FTO) (SnO_2F) and then grown on transparent conductive oxide (Alkauskas and Pasquarello, 2011; Ladanov *et al.,* 2011). ZnO nanowire was preferred to titanium dioxide because it is easier to be synthesized with different nanostructures compared. Also further advantages of ZnO nanowires over titanium dioxide includes the wider and direct bandgap (about 3.37 eV) compared to titanium dioxide (about 3.2eV), the excitation binding energy (60 meV) which is higher compared to 4 meV of titanium dioxide, and a higher electron mobility of about 200 $cm^3V^{-1}S^{-1}$ compared to titanium dioxide with 30 $cm^3V^{-1}S^{-1}$. Applying molecular beam epitaxy a narrow ZnO thin film was deposited uniformly on the silicon wafer. The temperature of the furnace was first raised to about 500 ^oC using a ramping rate fixed at 20^oC/min until attaining an optimal temperature. Then a steady flow of N_2 of 100 cm was blown into a tube while the pressure was kept constant at 1.0 x 10^{-2} Pa. Next, the furnace was cooled to a room temperature just after growth. The proposed developed product material was ZnO nanowires, well aligned with a high density. The product material was measured with 248 nm excimer, characterized using scanning electron microscopy and also photoluminescence spectroscopy.

2.4. The Ruthenium Complex Dye

The panchromatic ruthenium is a complex light harvesting sensitizer developed by combining carboxylate terpyridyl with three thiocyanate groups linked as ligands to achieve excellent incident photon conversion efficiencies in the solar cell (Kisserwan *et al.,* 2010; Chen et al., 2011; Islam *et al.,* 2011; Hallett *et al.,* 2011). The structure of the ruthenium complex dye is shown in Figure 2.

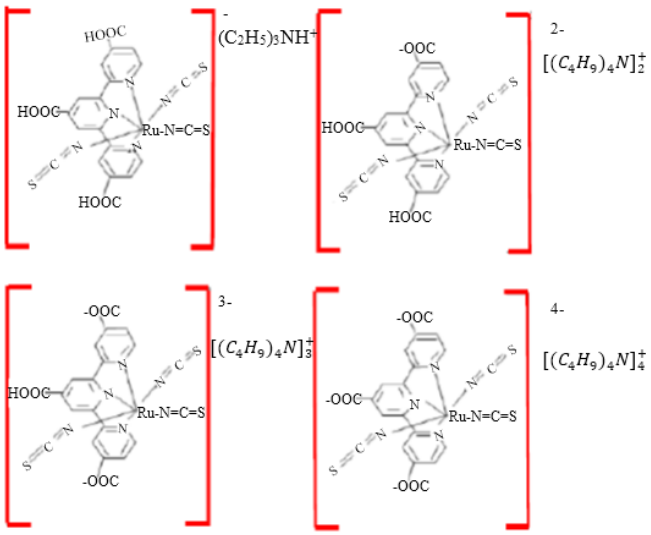

Figure 2: Ruthenium complex dye

The combination of the ruthenium dye and the isolated magnetosomes of MTB forms light harvesting trap with the ZnO nanowires. A structure consisting of two-dimensional pattern of a light harvesting system denoted as LH_1 in the outer shell and LH_2 in the inner shell was developed. These patterns consist of bounded photo-generated excitons transported integrated with magnetite of magnetosomes and driven by the inbuilt magnetic field to the donor acceptor interphase. The LH_1 system and the LH_2 system describes the integral MTB magnetosome proteins with magnetite in which all the generated exciton coupling pigments in the cell are organized regularly following repeated patterns in a circular order. A reaction center with a dense core surrounded circularly by the light harvesting LH_1 complex was created. Also the light harvesting LH_2 complexes patterns were arranged orderly around the surface perimeter of LH_1 ring following a 2D repeated structure. The reaction center was located within the center of ring LH_1. In that structure there exist over 5000 nanoparticles of magnetite in magnetosomes per enclosed reaction center. Each LH_1 unit was surrounded by over 10 LH_2 discrete units within the complex. Frenkel excitons were generated when light was absorbed following Frenkel's exciton model statistics. Theoretically the photo-generated exitons travel in unique coherent order in the described 2 dimensional light harvesting system to arrive the reaction center under the influence of the magnetic field of the magnetite. In the reaction center, the transition metal ion in the prosthetic group around a protein already is waiting to acquire the photon energy through received excitons to excite and dislocate an electron leading to series of electron transfer complex reaction (Fisher *et al.,* 2000; Wang *et al.,* 2003; Wang *et al.,* 2005). The entire photo-generated exciton transport system developed in the silicon solar cell is summarized in Figure 3.

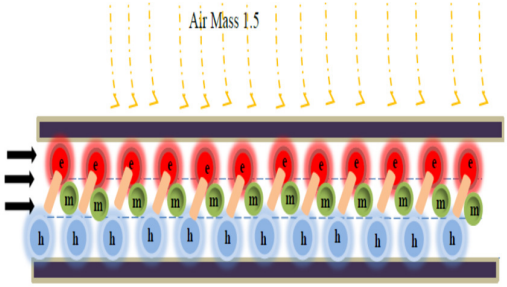

Figure 3: Photo-generated excitons being accelerated under the influence of nanoparticles of magnetite isolated from magnetosomes of magnetotactic bacteria

2.5. Theory

Solar cells are evaluated by the efficiency in the conversion of incident photons to electrical energy. In order to assess efficiency of the developed solar cell and focus on improving the step by step energy conversion process, emphasis was made on the light absorption of the device, charge transport, charge dissociation, and charge collection within the device, minimizing losses in a cost effective manner. Here we consider the following parameters:

$$\eta_{eff} = \eta_{abs} \text{ x } \eta_{dis} \text{ x } \eta_{trans} \text{ x } \eta_{col} \quad (1)$$

Where:

η_{eff} = total efficiency of Solar Cell
η_{abs} = the light absorption efficiency
η_{dis} = the generated exciton dissociation efficiency
η_{trans} = the charge carrier transport efficiency
η_{col} = the charge collection efficiency

Equation 1 describes how the generated charge carrier transport affects the total efficiency of the solar cell. Generally, the key factors of interest in photovoltaic cells performance include the open circuit voltage, short circuit current, fill factor, and maximum power. The power conversion efficiency (PCE) is defined as the ratio of the output power (P_{out}) of the solar cell to its input power (P_{in}) given by:

$$\text{Power} = \frac{P_{out}}{P_{in}} = \frac{J_{max}V_{max}}{P_{in}} = \frac{FFJ_{sc}V_{oc}}{P_{in}} \quad (2)$$

Where:

J_{max} is the Current density at maximum of (J x V)
J_{sc} = the Short circuit current
V_{oc} = the open circuit voltage
FF = the fill factor calculated

$$FF = \frac{J_m V_m}{J_{sc}V_{oc}} \quad (3)$$

Equations 2 and 3 were used to generate the efficiency of the developed solar cell applying the Labview toolkit VI. The total current voltage response of the solar cell can be approximated as the sum of the generated short circuit photocurrent and the dark current. The factor termed incident photon conversion efficiency (ICPE) is defined as the number of photo-generated charge carriers contributing to the photocurrent per incident photon.

3. RESULTS AND DISCUSSION

The developed excitonic photocell was tested with a LabVIEW toolkit at 25 ^{o}C. The characterization of the solar cell was done at standard conditions (irradiance 1000, W/m^2, air mass, 1.5). The results are presented in Figure 4 and compared with the result obtained from a dye sensitized solar cell without MTB under similar conditions in Figure 5. Accordingly, the proposed excitonic photocell shows a remarkable improvement in the fill factor achieving a value 0.82 compared to the dye sensitized solar cell value of 0.79. Also, the device efficiency improved, attaining a value of 13.2% attributed to the enhanced carrier transport. The results obtained using the LabVIEW toolkit VI is presented in Table 1.

U.I. Oduah / Nigerian Research Journal of Engineering and Environmental Sciences
4(1) 2019 pp. 389-397

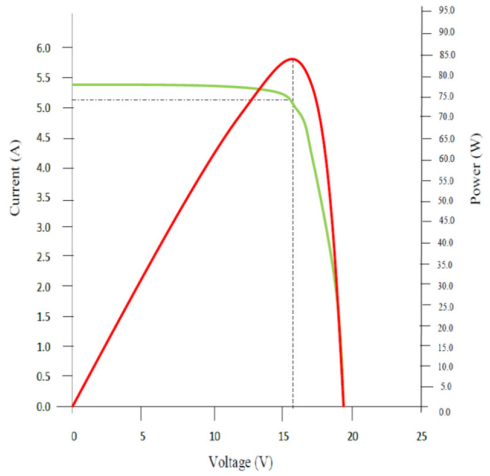

Figure 4: Plot of LabVIEW toolkit VI for characterization of the proposed excitonic photocell

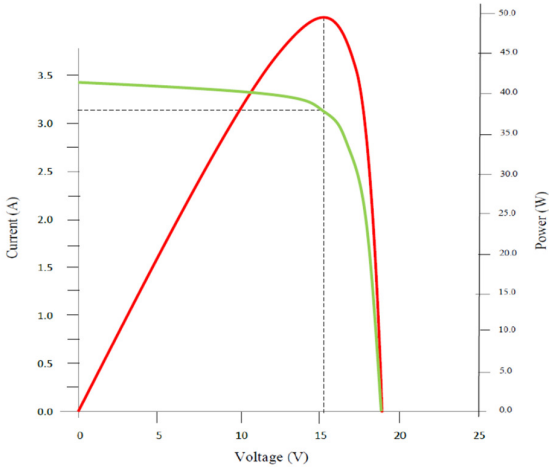

Figure 5: Plot of LabVIEW toolkit VI for characterization photovoltaic solar cell without MTB

Table 1: LabVIEW toolkit VI results and characterization of the developed excitonic photocell compared to dye sensitized solar cell

Parameter	Developed excitonic photocell	Dye sensitized solar cell
Light intensity (W/m^2)	1000	1000
Photon absorption area (m^2)	0.64	0.64
Short circuit current, I_{sc} (Amps)	5.41262	3.35342
Open circuit voltage, V_{oc} (Volts)	19.11315	18.17543
Fill factor, FF	0.816938	0.793154
Maximum power, P_{max} (watts)	84.51401	48.34263
Maximum voltage, V_{mp} (Volts)	16.21711	15.3121
Maximum current, I_{mp} (Amps)	5.21141	3.157152
Efficiency (%)	13.20531	7.55354

The parameters used in the characterization of the device are defined as follows.

Short Circuit Current (I_{sc}): This represents the short circuit condition when the impedance is low and is calculated when the voltage equals zero.

I (at $V = 0$) = I_{sc}

I_{sc} occurs at the beginning of the forward-bias sweep and is the maximum current value in the power quadrant. In ideal conditions, this maximum current value is the total current (I_t) produced in the device by photon excitation.

$I_{sc} = I_{max} = I_t$ for forward bias power quadrant.

Open circuit voltage (V_{oc}): This occurs when there is no current passing through the cell.

V (at $I = 0$) = V_{oc}

V_{oc} is also the maximum voltage difference across the cell for a forward-bias sweep in the power quadrant.

$V_{oc} = V_{max}$ for forward-bias power quadrant.

Maximum power (P_{max}) equals Current at P_{max} (I_{mp}) multiplied by Voltage at P_{max} (V_{mp}). The power produced by the device is given by $P = VI$. At the I_{sc} and V_{oc} points, the power is zero and the maximum value power is between the two points. The voltage and current at this maximum power point are denoted as V_{mp} and I_{mp} respectively. This novel coherent photo-generated carrier transport system enhanced the solar cell efficiency to a value 13.2%. Also, the device achieved temperature stability attributed to the uniformed speedy carrier transport mechanism.

There are concerns on the effect of temperature on the magnetic properties of magnetite. It is projected that an increase in temperature beyond the termed Curie temperature at (738 K), the resultant thermal fluctuations may destroy the normal ferromagnetic alignment feature of magnetic moments in magnetite. This may cause the ferromagnetic strength of the magnetite to diminish. At the Curie temperature, the net magnetization of a material drops to zero. But this is unlikely to occur in this case because the temperature of this device can never be elevated to such extreme temperatures during operation. The proposed excitonic photocell will also achieve higher thermostability attributed to the efficient coherent carrier transport mechanism.

4. CONCLUSION

This research developed a novel technology for the transportation of photo-generated excitons in the solar cell to achieve improved efficiency. In this work, it has been demonstrated that by integrating nanoparticles of magnetites isolated from magnetosomes of magnetotactic bacteria into the dye sensitized solar cell, the photo-generated carrier transport was enhanced. The coherent transport of the generated charges improved the efficiency of the solar cell. This novel technology has created a need to channel more attention to dye sensitized solar cells in order to maximize its potentials. Alternative sources of magnetite like chemical nanoparticles of magnetite have been observed not to have uniformed particle size making them unsuitable for this purpose. As part of processes towards commercialization of this technology, there is ongoing research targeted at producing nanoparticles of magnetite with uniformed particle size in a cost effective manner. Furthermore, there are considerations for the application of other dyes besides ruthenium complex like the MK-2 and MK-14 dyes. It is speculated that the efficiency of this developed device will achieve higher performance efficiencies exceeding that of silicon solar cells using other suitable light harvesting materials.

5. ACKNOWLEDGMENT

The author thanks the Physics Department and Microbiology Department of University of Lagos, for providing the facilities for this research project.

6. CONFLICT OF INTEREST

There is no conflict of interest associated with this work.

REFERENCES

Alkauskas A. and Pasquarello A. (2011). Band-edge problem in the theoretical determination of defect energy levels: the O vacancy in ZnO as a benchmark case. *Physical Review B,* 84, pp. 216-219.

Atlas R.M. (2010). *Handbook of Microbiological Media*. 4th Ed., pp. 994-997.

Benhattab S., Nakar R., Acosta R.J.W., Berton N., Faure-Vincent J., Bouclé J. and Schmaltz B. (2018). Carbazole-based twin molecules as hole-transporting materials in dye-sensitized solar cells. *Dyes and Pigments,* 151, pp. 238-244.

Change, W.C., Chen H.S. and Li T.Y. (2010). Highly efficient N-heterocyclic carbine/pyridine-based ruthenium sensitizers: complexes for dye-sensitized solar cells. *AngewandleChemie,* 49, pp. 8161-8167.

Chen, H.S., Chang, W.C. and Su, C. (2011). Carbene-based ruthenium photosensitizers. *Dalton Transactions,* 40, pp. 6765 – 6773.

Duerto, I., Colom, E., Andrés-Castán, J.M., Franco, S., Garín, J., Orduna, J. B., Villacampa, B. and Blesa M.J. (2018). DSSCs based on aniline derivatives functionalized with a *tert*-butyldimethylsilyl group and the effect of the π-spacer. *Dyes and Pigments,* 148, pp. 61-71.

Fisher, A.C., Peter, L.M., Ponomarev, E.A., Walker, A.B. and Wijayantha, K.G.U. (2000). Intensity dependence of the back reaction and transport of electrons in dye-sensitized nanocrystalline TiO_2 solar cells. *Journal of Physical Chemistry B,* 104, pp. 949-960.

Hallett, A.J. and Jones, J.E. (2011). Purification-free synthesis of a highly efficient ruthenium dye complex for dye-sensitised solar cells (DSSCs). *Dalton Transactions,* 40, pp. 3871-3879.

Islam, A., Singh, S.P., Yanagida, M., Karim, M.R. and Han, L. (2011). Amphiphilic ruthenium (II) terpyridine sensitizers with long alkyl chain substituted β-diketonato ligands: an efficient coadsorbent-free dye-sensitized solar cells. *International Journal of Photoenergy,* 2011, pp. 117-119.

Jobin, J.J. and Suthindhiran, K. (2016). Magnetotactic bacteria and magnetosomes – Scope and challenges. *Material Science and Engineering C,* 68, pp. 919-928.

Khan, M.Z.H., Al-Mamun, M.R., Halder, P.K. and Aziz, M.A. (2017). Performance improvement of modified dye-sensitized solar cells. *Renewable and Sustainable Energy Reviews,* 71, pp. 602-617.

Kisserwan, H. and Ghaddar, T.H. (2010). Enhancement of photovoltaic performance of a novel dye, "T 18", with ketene thioacetal groups as electron donors for high efficiency dye-sensitized solar cells. *InorganicaChimicaActa,* 363, pp. 2409-2418.

Kruger, J., Plass, R., Gratzel, M., Cameron, P.J. and Peter, L.M. (2003). Charge transport and back reaction in solid-state dye-sensitized solar cells; a study using intensity-modulated photovoltage and photocurrent spectroscopy. *Journal of Physical Chemistry B,* 107, pp. 7536-7542.

Ladanov, M., Ram, M.K., Matthews, G. and Kumar, A. (2011). Structure and opto-electrochemical properties of ZnO nanowires grown on n-Si substrate. *Langmuir,* 27, pp. 9012-9019.

Mahmoud, A. M., Abu, B. M., Norasikin, A.L., Amir, H.K. and Kamaruzzaman, S. (2016). Dye-sensitised solar cells: Development, structure, operation principles, electron kinetics, characterisation, synthesis materials and natural photosensitisers. *Renewable and Sustainable Energy Reviews,* 65, pp. 183-213.

Naik, P., Mohamed, R., Elmorsy, M.R., Su, R., Babu, D.D., El-Shafei, A. and Adhikari, A.V. (2017). New carbazole based metal-free organic dyes with D-π-A-π-A architecture for DSSCs: Synthesis, theoretical and cell performance studies. *Solar Energy,* 153, pp. 600-610.

Naik, P., Su, R., Elmorsy, M.R., El-Shafei, A. and Adhikari A.V. (2018). Investigation of new carbazole based metal-free dyes as active photo-sensitizers/co-sensitizers for DSSC's. *Dyes and Pigments,* 149, pp. 177-187.

Oduah, U.I. and Yang, W. (2016). Advanced Photodetector chip. *IEEE Sensor Journal*, 16, pp. 5610-5617.

Peng, G., Hoi, N., Joel, T. and Grätzel, M. (2018). Organic dyes containing fused acenes as building blocks: Optical, electrochemical and photovoltaic properties. *Chinese Chemical Letters*, 29, pp. 289-292.

Wadman, S.H., Kroon, J.M. and Bakker, K. (2011). Cyclometalated ruthenium complexes for sensitizing nanocrystalline TiO_2 solar cells. *Organic Chemistry & Catalysis,* 17, 24. pp. 6781-6790.

Wang, P., Wenger, B. and Humphry-Baker, R. (2005). Charge separation and efficient light energy conversion in sensitized mesoscopic solar cells based on binary ionic liquids. *Journal of the American Chemical Society,* 127, 18. pp. 6850-6859.

Wang, P. (2003). A stable quasi-solid-state dye-sensitized solar cell with an amphiphilic ruthenium sensitizer and polymer gel electrolyte. *Nature Material Science,* 2, pp. 402-410.

Zhu, K., Pan, H., Li, J., Yu-Zhang, K., Zhang, S., Zhang, W., Zhou, K., Yue, H., Pan, Y., Xiao, T. and Wu, L. (2010). Isolation and characterization of a marine magnetotactic spirillum axenic culture QH-2 from an intertidal zone of the China Sea. *Research in Microbiology,* 161, pp. 276-283.